



Calhoun: The NPS Institutional Archive
DSpace Repository

Theses and Dissertations

1. Thesis and Dissertation Collection, all items

2002-06

Improved aerothermodynamic instrumentation of an Allison T63-A-700 gas turbine engine

Bruan, Kenneth C.

Monterey, California. Naval Postgraduate School

<http://hdl.handle.net/10945/5956>

This publication is a work of the U.S. Government as defined in Title 17, United States Code, Section 101. Copyright protection is not available for this work in the United States.

Downloaded from NPS Archive: Calhoun



<http://www.nps.edu/library>

Calhoun is the Naval Postgraduate School's public access digital repository for research materials and institutional publications created by the NPS community. Calhoun is named for Professor of Mathematics Guy K. Calhoun, NPS's first appointed -- and published -- scholarly author.

Dudley Knox Library / Naval Postgraduate School
411 Dyer Road / 1 University Circle
Monterey, California USA 93943

NAVAL POSTGRADUATE SCHOOL

Monterey, California



THESIS

**IMPROVED AEROTHERMODYNAMIC
INSTRUMENTATION OF AN ALLISON T63-A-700 GAS
TURBINE ENGINE**

by

Kenneth C. Bruan

June 2002

Thesis Advisor:

K. T. Millsaps

Approved for public release; distribution is unlimited.

THIS PAGE INTENTIONALLY LEFT BLANK

REPORT DOCUMENTATION PAGE			Form Approved OMB No. 0704-0188	
Public reporting burden for this collection of information is estimated to average 1 hour per response, including the time for reviewing instruction, searching existing data sources, gathering and maintaining the data needed, and completing and reviewing the collection of information. Send comments regarding this burden estimate or any other aspect of this collection of information, including suggestions for reducing this burden, to Washington headquarters Services, Directorate for Information Operations and Reports, 1215 Jefferson Davis Highway, Suite 1204, Arlington, VA 22202-4302, and to the Office of Management and Budget, Paperwork Reduction Project (0704-0188) Washington DC 20503.				
1. AGENCY USE ONLY (Leave blank)		2. REPORT DATE June 2002	3. REPORT TYPE AND DATES COVERED Master's Thesis	
4. TITLE AND SUBTITLE: Title (Mix case letters) IMPROVED AEROTHERMODYNAMIC INSTRUMENTATION OF AN ALLISON T63-A-700 GAS TURBINE ENGINE			5. FUNDING NUMBERS	
6. AUTHOR(S) Kenneth C. Bruan				
7. PERFORMING ORGANIZATION NAME(S) AND ADDRESS(ES) Naval Postgraduate School Monterey, CA 93943-5000			8. PERFORMING ORGANIZATION REPORT NUMBER	
9. SPONSORING / MONITORING AGENCY NAME(S) AND ADDRESS(ES) N/A			10. SPONSORING/MONITORING AGENCY REPORT NUMBER	
11. SUPPLEMENTARY NOTES The views expressed in this thesis are those of the author and do not reflect the official policy or position of the Department of Defense or the U.S. Government.				
12a. DISTRIBUTION / AVAILABILITY STATEMENT Approved for public release, distribution is unlimited			12b. DISTRIBUTION CODE	
13. ABSTRACT (maximum 200 words) <p>This document describes the design, installation, and operation of an improved measurement system for the aerothermodynamic flow path states in an Allison T63-A-700 (C250-18 civilian designation). Temperature measurements for the gas generator turbine and exhaust state points were evaluated and average values were calculated. The measurement uncertainty for airflow, fuel flow, and output power has been reduced to less than 3%. State points match installation design data within 3%. The digital scanning array has improved the accuracy of the pressure measurements and added the ability to measure pressure differences over time. The added bellmouth pressure sensors provide a redundant pressure measurement that is more accurate than the dynamometer system. The gas generator turbine inlet and exhaust temperature profiles have been measured and show that the temperature profile becomes less symmetrical with increasing air and fuel flow. The measurement values for the gas generator inlet temperature have been consolidated into a single value that is about 50 degrees different from expected values. The temperature profile at the power turbine inlet shows how the hot spot at the gas generator turbine inlet is affected by the swirl produced by the power turbine stages. The time resolved fluctuations in pressure between the compressor and gas generator turbine have been measured and show that compressor discharge and gas generator turbine inlet pressures are similar.</p>				
14. SUBJECT TERMS aerothermodynamic instrumentation, gas turbine engine, gas generator turbine inlet			15. NUMBER OF PAGES 58	
			16. PRICE CODE	
17. SECURITY CLASSIFICATION OF REPORT Unclassified	18. SECURITY CLASSIFICATION OF THIS PAGE Unclassified	19. SECURITY CLASSIFICATION OF ABSTRACT Unclassified	20. LIMITATION OF ABSTRACT UL	

THIS PAGE INTENTIONALLY LEFT BLANK

Approved for public release; distribution is unlimited

**IMPROVED AEROTHERMODYNAMIC INSTRUMENTATION OF AN
ALLISON T63-A-700 GAS TURBINE ENGINE**

Kenneth C. Bruan
Ensign, United States Navy
B.S.M.E., University of Memphis, 2001

Submitted in partial fulfillment of the
requirements for the degree of

MASTER OF SCIENCE IN MECHANICAL ENGINEERING

from the

**NAVAL POSTGRADUATE SCHOOL
June 2002**

Author: Kenneth C. Bruan

Approved by: Knox T. Millsaps
Thesis Advisor

Terry R. McNelley, Chairman
Department of Mechanical Engineering

THIS PAGE INTENTIONALLY LEFT BLANK

ABSTRACT

This document describes the design, installation, and operation of an improved measurement system for the aerothermodynamic flow path states in an Allison T63-A-700 (C250-18 civilian designation). Temperature measurements for the gas generator turbine and exhaust state points were evaluated and average values were calculated. The measurement uncertainty for airflow, fuel flow, and output power has been reduced to less than 3%. State points match installation design data within 3%. The digital scanning array has improved the accuracy of the pressure measurements and added the ability to measure pressure differences over time. The added bellmouth pressure sensors provide a redundant pressure measurement that is more accurate than the dynamometer system. The gas generator turbine inlet and exhaust temperature profiles have been measured and show that the temperature profile becomes less symmetrical with increasing air and fuel flow. The measurement values for the gas generator inlet temperature have been consolidated into a single value that is about 50 degrees different from expected values. The temperature profile at the power turbine inlet shows how the hot spot at the gas generator turbine inlet is affected by the swirl produced by the power turbine stages. The time resolved fluctuations in pressure between the compressor and gas generator turbine have been measured and show that compressor discharge and gas generator turbine inlet pressures are similar.

THIS PAGE INTENTIONALLY LEFT BLANK

TABLE OF CONTENTS

I.	INTRODUCTION	1
A.	BACKGROUND	1
B.	MOTIVATION	2
C.	OBJECTIVES	2
D.	ORGANIZATION	2
II.	ENGINE DESCRIPTION AND THERMODYNAMIC MODEL ANALYSIS.....	5
A.	ENGINE DESCRIPTION	5
B.	THERMODYNAMIC MODEL ANALYSIS	6
III.	INITIAL MEASUREMENT SYSTEM, MEASUREMENT PROBLEMS, AND INSTRUMENTATION REQUIREMENTS	13
A.	INITIAL MEASUREMENT SYSTEM	13
B.	MEASUREMENT PROBLEMS.....	14
1.	Lack of Compressor Inlet Pressure Measurement	14
2.	Pressure Measurement Instrumentation.....	14
3.	Gas Generator Inlet Temperature	15
4.	Exhaust Temperature	16
C.	INSTRUMENTATION REQUIREMENTS	16
IV.	INSTRUMENTATION IMPROVEMENTS	19
A.	PRESSURE SENSOR SYSTEM REPLACEMENTS	19
B.	IMPLEMENTATION	21
C.	TEMPERATURE INSTRUMENTATION	21
V.	RESULTS AND EVALUATION	23
A.	KEY PARAMETERS.....	23
B.	STATE POINT MEASUREMENTS	24
C.	GAS GENERATOR TURBINE INLET TEMPERATURE PROFILE...24	
D.	EXHAUST TEMPERATURE.....	26
E.	PRESSURE MEASUREMENTS	27
VI.	SUMMARY, CONCLUSIONS AND RECOMMENDATIONS	31
	APPENDIX A. DSA 3017 SPECIFICATIONS.....	35
	APPENDIX B. MATLAB CODE FOR GGT INLET TEMPERATURE PROFILE	37
	APPENDIX C. COLLECTED DATA	39
	LIST OF REFERENCES	41
	INITIAL DISTRIBUTION LIST.....	43

THIS PAGE INTENTIONALLY LEFT BLANK

LIST OF FIGURES

Figure 2.1.	Model 250 Gas Turbine Engine. [From Ref 3].....	6
Figure 2.2.	Engine Schematic. [After Ref 3]	10
Figure 2.3.	Calibrated model T-s diagram	12
Figure 4.1.	Scanivalve DSA 3017 Pressure Sensor	19
Figure 4.2.	DSA 3017 Schematic [Top View].....	20
Figure 5.1.	Gas generator turbine inlet profile factor @ 80% of maximum compressor speed	25
Figure 5.2.	Gas generator turbine inlet profile factor @ 100% of maximum compressor speed.....	26
Figure 5.3.	Power turbine exit temperature measurements at constant gas generator turbine speed for 5 different power turbine speeds	27
Figure 5.4.	Compressor discharge pressure measurement fluctuations	28
Figure 5.5.	Gas generator inlet pressure measurement fluctuations	29
Figure 5.6.	Compressor discharge and gas generator inlet pressure measurement fluctuation comparison	29

THIS PAGE INTENTIONALLY LEFT BLANK

LIST OF TABLES

Table 2.1. Installation design manual data, standard inlet model and calibrated model comparison.....	11
Table 4.1. Pressure Sensor Locations	20
Table 4.2. Temperature Sensor Locations	21
Table 5.1. Key parameter comparison.....	23
Table 5.2. State point comparison	24
Table 5.3. Gas generator turbine inlet temperature comparison @ full power	25
Table 5.4. Compressor adiabatic efficiency comparison.....	28
Table C.1. Temperature and pressure data	39

THIS PAGE INTENTIONALLY LEFT BLANK

NOMENCLATURE

<u>Symbol</u>	<u>Description</u>	<u>Units</u>
\bar{c}_p	Specific heat	[BTU/lbm-°R]
f	fuel to air ratio	[1]
\dot{m}_a	Air mass flow rate	[lbm/s]
\dot{m}_f	Fuel mass flow rate	[lbm/hr]
N1	Compressor / Gas generator turbine speed	[rpm]
N1 _c	Corrected compressor speed	[rpm]
N2	Power turbine speed	[rpm]
N3	Output shaft speed	[rpm]
P _{heatloss}	Heat rejection to oil	[BTU/min]
P _{out}	Output power	[hp]
P ₂	Compressor inlet static pressure	[psia]
P _{t2}	Compressor inlet total pressure	[psia]
P _{t3}	Compressor inlet total pressure	[psia]
P _{t4}	Gas generator turbine inlet total pressure	[psia]
P _{t5}	Power turbine inlet total pressure	[psia]
P _{t7}	Power turbine exit total pressure	[psia]
Q _R	Fuel lower heating value	[BTU/lbm]
T _{t2}	Compressor inlet total temperature	[°R]
T _{t3}	Compressor discharge total pressure	[°R]
T _{t4}	Gas generator turbine inlet total temperature	[°R]
T _{t5}	Power turbine inlet total temperature	[°R]

<u>Symbol</u>	<u>Description</u>	<u>Units</u>
T_{t7}	Power turbine exit total temperature	[°R]
η_c	Compressor adiabatic efficiency	[1]
η_{ggt}	Gas generator turbine adiabatic efficiency	[1]
η_{pt}	Power turbine adiabatic efficiency	[1]
$\pi_b = P_{t4}/P_{t3}$	Combustor pressure ratio	[1]
$\pi_c = P_{t3}/P_{t2}$	Compressor pressure ratio	[1]
$\pi_{\text{ggt}} = P_{t5}/P_{t4}$	Gas generator turbine pressure ratio	[1]
$\pi_{\text{pt}} = P_{t7}/P_{t5}$	Power turbine pressure ratio	[1]
ρ	Density	[lbm/ft ³]
$\tau_c = T_{t3}/T_{t2}$	Compressor temperature ratio	[1]
$\tau_{\text{ggt}} = T_{t5}/P_{t4}$	Gas generator turbine temperature ratio	[1]
$\tau_{\text{pt}} = T_{t7}/P_{t5}$	Power turbine temperature ratio	[1]

I. INTRODUCTION

A. BACKGROUND

Gas turbine engines are commonly used to produce electrical and propulsive power for surface and airborne craft in the United States Navy. It is important for Naval Officers to be familiar with gas turbine engines because many shipboard jobs involve operating and maintaining them.

At the Naval Postgraduate School, courses such as Marine Power and Propulsion (ME3240) give students the opportunity to apply theory presented in class on a fully operational gas turbine. The hands on experience allows students to see how each major component operates and interacts with the entire system. Thermodynamic theory of the Brayton cycle can be compared to measured values in an operating engine.

The engine currently in use in this lab is the Allison T63-A-700 gas turbine, which has a C250-C18 civilian designation. Brian Eckerle [Ref 4] attached the engine to a dynamometer system that measures key parameters like airflow, fuel flow, and output power. David Haas [Ref 3] designed, built, and installed an instrumentation package to analyze the performance of the gas turbine and its major components, because the original engine instrumentation was insufficient. This package consists of pressure probes and thermocouples placed between major components, to measure temperature and pressure of the air throughout the engine.

Calculations made with measurements from Haas' instrumentation package did not match values from the installation design manual, due to three major discrepancies. First, some of the pressure sensors were not installed and others were giving incorrect values. Second, measured values for airflow, fuel flow and output power varied as much as 10%-15% from installation design values. As a result, component adiabatic efficiency calculations were too high to be representative of a realistic model. Third, the gas generator inlet and power turbine exit temperatures were measured with numerous devices, but their average values did not match temperatures calculated by energy balances. Since these temperatures are critical for an accurate thermodynamic cycle analysis, their proper formulation demands closer attention.

B. MOTIVATION

Increasing the quality of the measurements for the ME3240 gas turbine laboratory motivated this thesis. Matching measurements with values based on the installation design manual appeared to be a practical method for evaluating and interpreting data.

C. OBJECTIVES

The objectives of this thesis are assessing the quality and reliability of the current measurement system; creating a plan for improving measurements; designing, fabricating, and installing an improved package, and evaluating the improved measurements.

D. ORGANIZATION

Chapter II describes the engine, its major components, and general performance data. A thermodynamic model is presented, based on installation design values at standard inlet conditions, which predicts the component adiabatic efficiencies. These component adiabatic efficiencies are used in a calibrated model to predict the thermodynamic states through the engine for non-standard inlet conditions, which is used to evaluate the measurement based model.

Chapter III describes the measurement assessment. Problems with instrumentation giving inaccurate measurements are explained. Determinations whether the faulty data are due to missing devices, broken instrumentation, or an incorrect analysis of the measurements are made. Measurement requirements are also listed.

Chapter IV explains the improved measurement plan. The design, manufacture, and installation of the improved measurement system are described. The implementation of this new plan is shown.

Chapter V presents the results and an evaluation of the improvements. The new measurement data are compared with design values. New averaged values for gas generator inlet temperature and exhaust temperature are explained.

Chapter VI summarizes the work that has been done, provides conclusions that have been drawn from comparisons between values predicted in the thermodynamic model and measurements, identifies existing problems and proposes further work to settle unsolved discrepancies.

THIS PAGE INTENTIONALLY LEFT BLANK

II. ENGINE DESCRIPTION AND THERMODYNAMIC MODEL ANALYSIS

A. ENGINE DESCRIPTION

An Allison Model C250-C18 (T63-A-700 military) gas turbine engine is installed in the Marine Propulsion Laboratory. The Allison Division of the now Rolls Royce Corporation produced this engine. Its primary use in the military was propulsion for the U.S. Army's OH-58 light observation helicopter. With over 25,000 made, and more than 5,000 shipped to the U.S. Military, the Allison C250 is one of the most commonly produced gas turbines. Weighing 138 pounds, this twin spool free power turbine engine has the ability to produce 317 shaft horsepower (SHP) at standard conditions (59° F, 1 ATM) with a compressor speed at 105%. Its gas generator turbine is rated at 51,120 RPM (100%) and its power turbine is rated at 35,000 (100%), which is geared to 6,000 RPM. The specific fuel consumption for maximum continuous power is rated at 0.708 lbm/SHP-hr. The gas turbine engine is rated at 304 shaft horsepower at 100% gas generator turbine and 100% power turbine speed with standard inlet conditions.

This gas turbine engine consists of four major components: the compressor, the combustor, the gas generator turbine, and the power turbine. Air enters the engine through the compressor. It passes through six axial compressor stages into a 7th stage, which is centrifugal. At standard temperature and pressure inlet, and at maximum power, the compressor pressure ratio is rated at 6.149:1. The air exits the compressor through two scroll type diffusers. Two circular ducts direct the air to the combustor, which is located at the rear of the engine. As the air enters the combustor, it reverses direction while the single fuel nozzle injects fuel into the flow.

The combustion gas then passes through the gas generator turbine's (GGT) two axial stages. The power produced by the gas generator drives the compressor and engine accessories. The flow then passes through the two axial stage power turbine (PT). The power turbine is connected to a helical reduction gear, which drives a variable speed output shaft. The engine type is typically run at a constant speed with variable torque,

but the specific engine used in this laboratory has been modified so the speed could be varied.

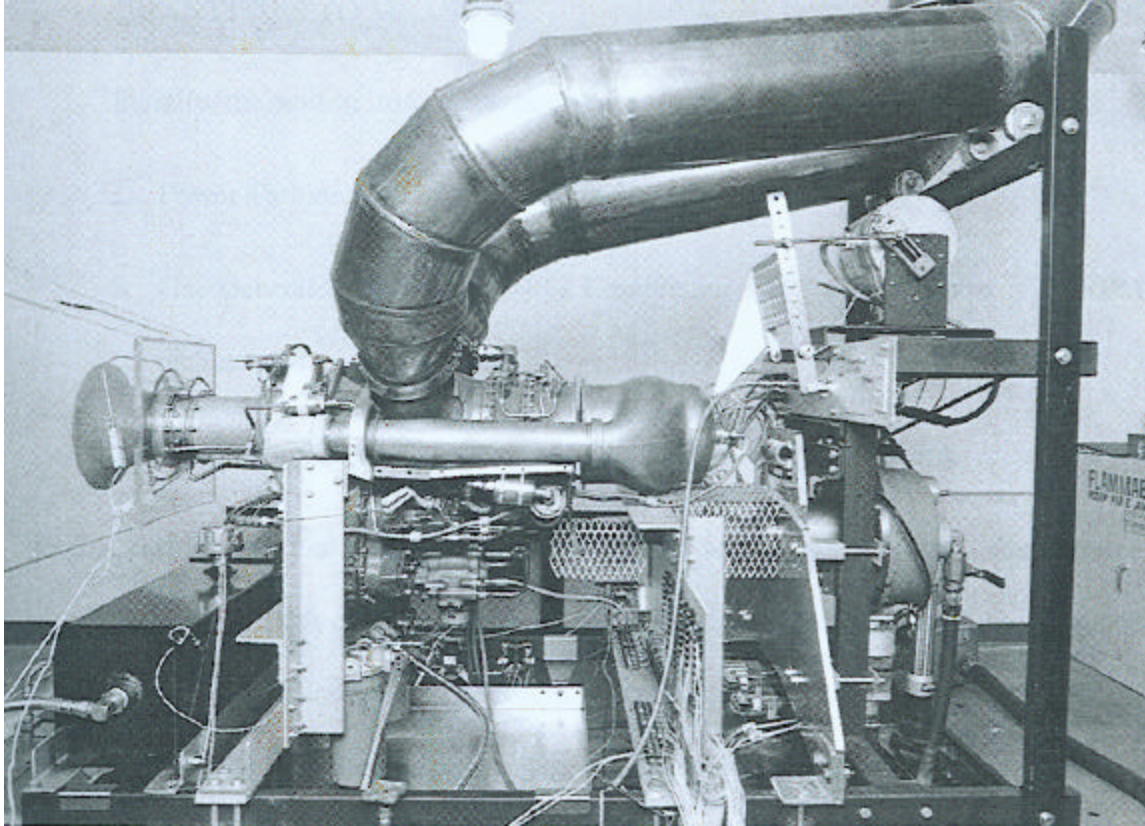


Figure 2.1. Model 250 Gas Turbine Engine. [From Ref 3]

B. THERMODYNAMIC MODEL ANALYSIS

The thermodynamic cycle analysis provided below was done to describe the state of the working fluid at the inlet and exhaust of every component, for a comparison between measurement data and installation design values. The analysis is done at full power: $N1=100\%$, $N2=100\%$. Five major inter-component locations are considered when analyzing the gas turbine thermodynamic cycle. These points are the compressor inlet (2), the compressor discharge (3), GGT inlet (4), PT inlet (5), and the exhaust (7).

The installation design manual was used to formulate a calibrated model for comparison with a measurement based model. The installation design manual was used

to provide values for a standard inlet model, but the data did not include all of the required parameters. The values from the installation design manual for standard inlet conditions include [Ref 1]:

1. Output shaft horsepower (SHP = 304 hp)
2. Gas generator turbine exit temperature ($T_{t5} = 1815$ R)
3. Fuel flow rate ($\dot{m}_f = 210$ lbm/hr)
4. Airflow rate ($\dot{m}_a = 3.13$ lbm/s)
5. Compressor discharge total temperature ($T_{t3} = 964$ R)
6. Compressor discharge total pressure ($P_{t3} = 90.37$ psia)
7. Oil heat rejection ($P_{\text{heatloss}} = 13.44$ hp)

Some parameter values were assumed for the calculations required to complete the analysis. Experimental data from Appendix C of was used to estimate the following values with the exception of the gear box efficiency. The values that were assumed include:

1. Combustor total pressure ratio ($p_b = 0.973$)
2. Gas generator turbine total pressure ratio ($p_{\text{ggt}} = 0.377$)
3. Gear box efficiency ($h_{\text{gb}} = 0.920$)

Values from the installation design manual were used with the assumed parameters to calculate the following values needed to finish the standard inlet model.

1. Gas generator turbine inlet total temperature
2. Power turbine exit total temperature
3. Compressor adiabatic efficiency
4. Gas generator turbine adiabatic efficiency

5. Power turbine adiabatic efficiency

A fuel based calculation for gas generator turbine inlet temperature was made with values from the installation design manual. The values required are the compressor discharge total temperature (T_{t3}), the fuel to air ratio ($f = \dot{m}_a / \dot{m}_f$), the lower heating value for the fuel ($Q_R = 18400$ BTU/lbm), and the average specific heat across the combustor.

$$T_{t4} = \frac{\bar{c}_{p,burner} T_{t3} + f Q_R}{(1 + f) \bar{c}_{p,burner}} \quad (2.1)$$

A design value for the power turbine exit temperature was calculated by evaluating an energy balance across the PT using the gearbox efficiency.

$$SHP = ((\dot{m}_a + \dot{m}_f) (T_{t5} - T_{t7}) \bar{c}_{ppt}) \cdot h_{gearbox} \quad (2.2)$$

The compressor adiabatic efficiency, η_c , is given by

$$h_c = \frac{p_c^{\frac{g-1}{g}} - 1}{t_c - 1} \quad (2.3)$$

where π_c is the total pressure ratio between the compressor discharge and inlet, and τ_c is the total temperature ratio between the compressor discharge and inlet.

The gas generator turbine adiabatic efficiency, η_{ggt} , is given by

$$h_{ggt} = \frac{1 - t_{ggt}^{\frac{g-1}{g}}}{1 - p_{ggt}^{\frac{g-1}{g}}} \quad (2.4)$$

where π_{ggt} is the total pressure ratio between the gas generator turbine exit and inlet, and τ_{ggt} is the total temperature ratio between the gas generator turbine exit and inlet.

The total to static power turbine adiabatic efficiency, η_{pt} , is given by

$$h_{pt} = \frac{1 - \tau_{pt}}{1 - \pi_{pt}^{\frac{\gamma-1}{\gamma}}} \quad (2.5)$$

where π_{pt} is the ratio between the power turbine exit static pressure and inlet total pressure, and τ_{pt} is the total temperature ratio between the power turbine exit and inlet.

After the standard inlet condition model calculations were completed, values from the installation design manual for non-standard inlet conditions were used with the component adiabatic efficiencies from the standard inlet model to calculate the state points values for a calibrated model that are not given by the installation design manual. These are the guidelines used for calculating the state points for the calibrated model.

1. Compressor inlet conditions were matched with experimental measurements.
2. Compressor discharge conditions were obtained from the installation design manual.
3. Gas generator inlet pressure was calculated by using the estimated combustor pressure ratio and the temperature was calculated by using equation 2.1.
4. Power turbine inlet temperature was obtained from the installation design manual and the pressure was calculated by using the gas generator turbine adiabatic efficiency from the standard inlet model with equation 2.4.
5. Power turbine exit temperature was calculated by using equation 2.2 with the estimated gear box efficiency and installation design values. The pressure was calculated by using the power turbine adiabatic efficiency with equation 2.5.

The values from the calibrated model will be used to evaluate the instrumentation measurement data. Note that the compressor adiabatic efficiency for the non standard model was recalculated because all the required values were in the installation design manual.

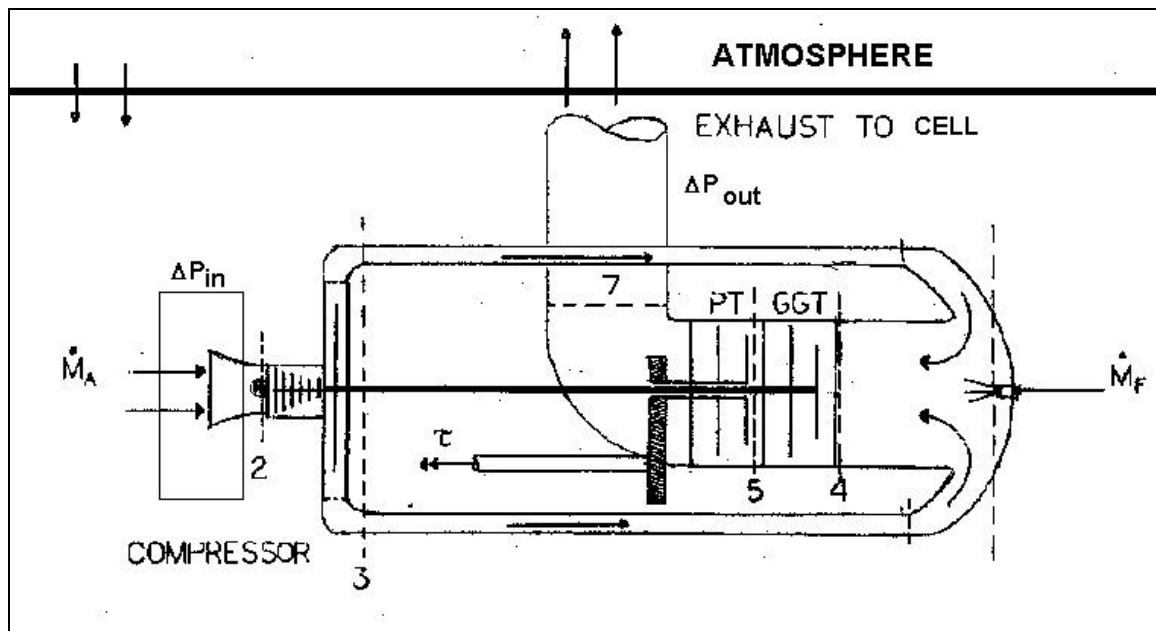


Figure 2.2. Engine Schematic. [After Ref 3]

Table 2.1. Installation design manual data, standard inlet model and calibrated model comparison

	P_{t1}	ΔP_{loss}	P_{t2}	P_{t3}	π_c	π_b	P_{t4}	π_{ggt}	P_{t5}	P_{t7}
	[psia]	[psia]	[psia]	[psia]			[psia]		[psia]	[psia]
IDM @ ISO	14.696	0.000	14.696	90.370	6.149	N/A	N/A	N/A	N/A	N/A
Standard Model	14.696	0.000	14.696	90.370	6.149	0.970	87.659	0.377	33.047	14.696
IDM @ non ISO	N/A	N/A	14.591	83.980	5.756	NA	NA	N/A	N/A	N/A
Calibrated Model	14.681	0.090	14.591	83.980	5.756	0.970	78.101	0.380	29.640	14.702

	T_{t2}	T_{t3}	τ_c	T_{t4}	T_{t5}	T_{t7}		η_c	η_{ggt}	η_{pt}
	[R]	[R]		[R]	[R]	[R]				
IDM @ ISO	519.0	964.0	1.857	N/A	1815.0	N/A		0.793	N/A	N/A
Standard Model	519.0	964.0	1.857	2216.7	1815.0	1533.3		0.793	0.745	0.7509
IDM @ non ISO	535.0	980.0	1.832	N/A	1830.0	N/A		0.780	N/A	N/A
Calibrated Model	535.0	980.0	1.832	2232.7	1830.0	1565.2		0.780	0.745	0.751

	N_1	N_{1c}	P_{out}	air flow	fuel flow	SFC	Q_R
	[rpm]	[rpm]	[hp]	[lbm/s]	[lbm/hr]	[lbm/hr/hp]	[BTU/lbm]
IDM @ ISO	51200	51200	304.00	3.13	210.00	0.691	18400
Standard Model	51200	51200	304.00	3.13	210.00	0.691	18400
IDM @ non ISO	51200	50429	285.94	3.02	202.54	0.708	18566
Calibrated Model	51200	50429	285.94	3.02	202.54	0.708	18566

This table contains parameters necessary to perform the thermodynamic cycle analysis, shown as two sets of data. The first set is for standard inlet conditions and occupies the first two rows. The first row is taken directly from the installation design manual, and the second row adds a few values (calculated from first row parameters) to complete the chart.

The second set, in the next two rows, is for non-standard inlet conditions. These inlet conditions are chosen to match those present for a majority of the experimental runs. Parameters in the third row are calculated using component adiabatic efficiencies determined from the data in the first set, and the non-standard inlet conditions (535 °R, 14.681 psia). Fourth row calculations use third row data to complete the chart.

There is an inlet loss due to the pressure drop from the ambient condition to the compressor inlet, and there is a backpressure at the exhaust because of the ducting between the cell and the atmosphere. At the same compressor speed, the increase of inlet temperature will decrease the tangential Mach number of the compressor blades and the compressor pressure ratio will be lower. There is a decrease in compressor temperature ratio, which would result in a lower pressure ratio at a constant adiabatic efficiency. Figure 2.3 shows how work is lost due to the inlet pressure loss, the backpressure, and the increase in inlet temperature.

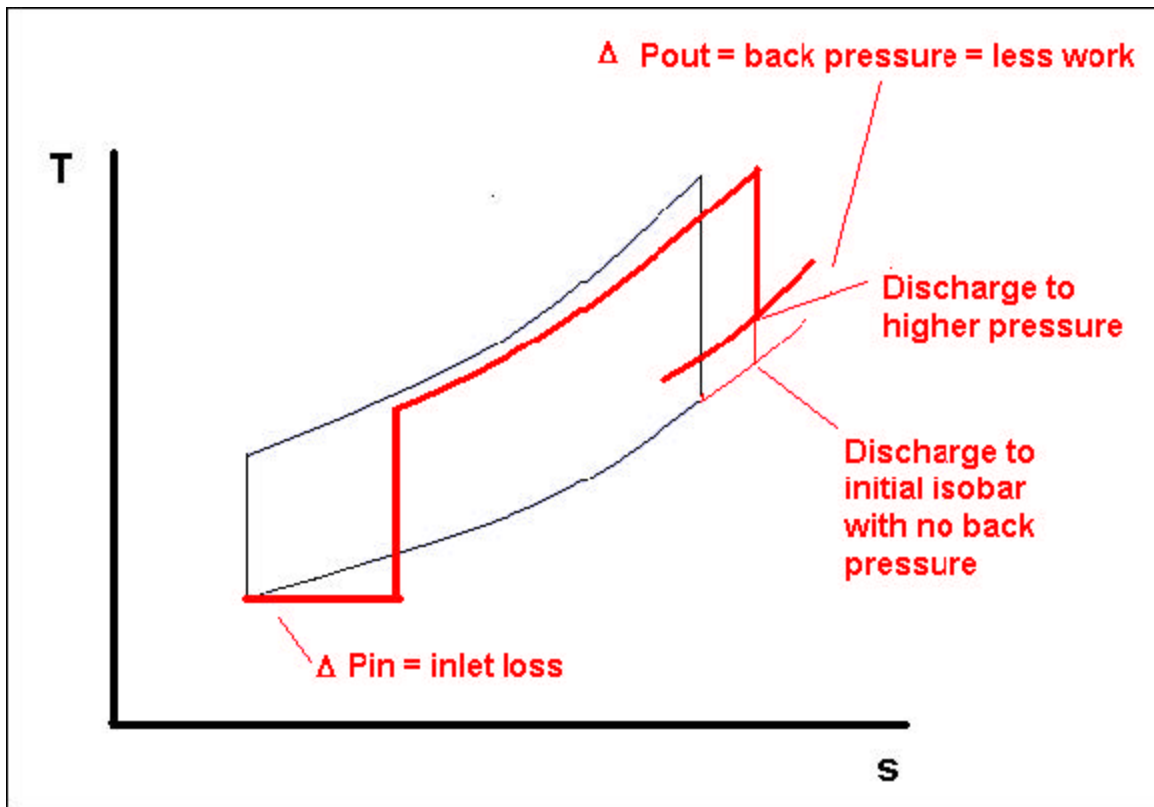


Figure 2.3. Calibrated model T-s diagram

III. INITIAL MEASUREMENT SYSTEM, MEASUREMENT PROBLEMS, AND INSTRUMENTATION REQUIREMENTS

A. INITIAL MEASUREMENT SYSTEM

The instrumentation that was installed the Allison Corporation took three measurements. The values that were measured included:

- | | | | |
|----|---------------------------------|-------|-----------------|
| 1. | Power Turbine Inlet Temperature | [F] | T _{t5} |
| 2. | Compressor Speed | [rpm] | N1 |
| 3. | Power Turbine Speed | [rpm] | N2 |

The instrumentation that was included with the Superflow 901 Dynamometer system measured the output parameters and auxiliary system conditions. The values that were measured are:

- | | | |
|----|--------------------|----------|
| 1. | Air Flow | [scfm] |
| 2. | Fuel Flow | [lbm/hr] |
| 3. | Output Shaft Speed | [rpm] |
| 4. | Torque | [ft-lbf] |
| 5. | Fuel Temperature | [F] |
| 6. | Oil Temperature | [F] |

The dynamometer also has the ability to calculate brake specific fuel consumption [BSFC], brake specific air consumption [BSAC], air to fuel ratio [A/F], and output shaft horsepower. The humidity can be entered into the dynamometer system for corrected parameter values for output shaft speed and horsepower. The specific gravity of the fuel has to be entered for the fuel flow measurement. The vapor pressure of the atmosphere has to be entered for an accurate measurement of airflow.

The temperature measurements were taken with thermocouples that are connected to a Hewlett Packard 3852A Data Acquisition Control Unit for signal processing. A

single transducer near the measurement location was used to measure each pressure value. Due to the non-uniform velocities within the flow, finding the bulk average measurements of the flow was important in designing the instrumentation package.

B. MEASUREMENT PROBLEMS

1. Lack of Compressor Inlet Pressure Measurement

There were no pressure measurements at the compressor inlet. The pressure loss through the ducting and the plenum would have to be determined for an accurate calculation for the compressor inlet total and static pressures.

2. Pressure Measurement Instrumentation

Omega pressure transducers were installed throughout the gas turbine system to start operation of the gas turbine laboratory. These pressure transducers were inexpensive and not well made. The pressure devices were installed six years ago and the several failures prove that it is time for an overhaul.

There were two scales for the pressure transducers used, 50-psid and 100-psid. Appropriate transducers were used at measurement locations throughout the engine, except at the exhaust. Two 50-psid pressure transducers were used to measure a differential pressure of half of a psid. The scale of the transducers was too high for the measurement range. The pressure transducer's output signal is in volts, and if the measurement range is a small percentage of the instrument's scale, the output signal will be on the order of signal noise. It was difficult to get consistent data from these two transducers and it became clear that it is important to match instrumentation scale to measurement range.

Temperature and pressure measurements were taken sequentially meaning that the measurement at each state point may not correspond to the next point. This snapshot of data is not representative of the flow because of fluctuations caused by its temporal variations. The variations in compressor speed cause the pressure measurements to change over time. The temperature measurements are not affected as much as the

pressure measurements because of thermal inertia, there is a lag between the change in compressor speed and the temperature measurement. The data could include a measurement spike that would be greatly different from the averaged value. A time-averaged value over several minutes would give a more accurate measurement.

3. Gas Generator Inlet Temperature

Due to the great non-uniformity of the flow velocity and the combustion within the combustor, a wide range of temperatures can be experienced and their distribution would be difficult to predict. That is why a large number of thermocouples were used to evaluate this condition.

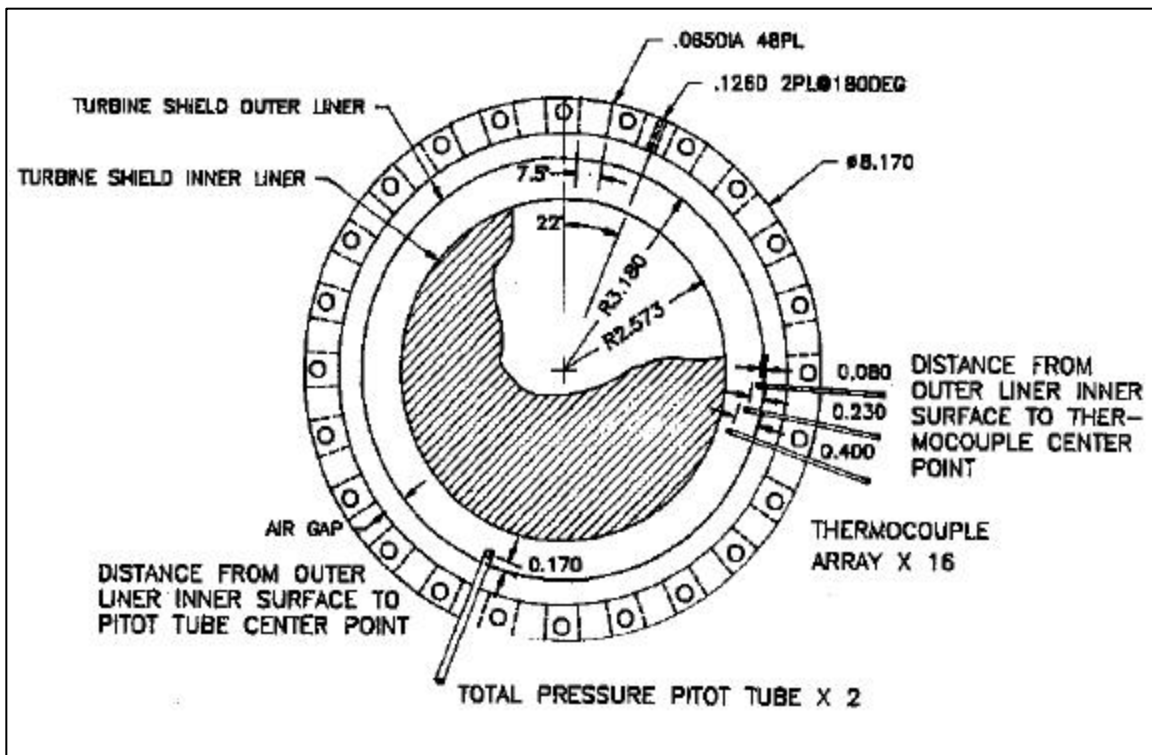


Figure 3.1. Schematic of gas generator instrumentation ring [From Ref 3]

A mass based value gives a representative bulk average because the variation of temperature and fluid condition at every measurement point is taken into account. An analysis of a mass based enthalpy average utilized the fact that the thermocouples at the

blade tips accounted for a smaller cross sectional area, the location of the maximum temperatures.

Evaluating the specific heat, temperature, and density of all forty-eight thermocouples refines the analysis. Finding the velocity profile through the annulus would require many measurements, which would increase losses from instruments that can be easily clogged.

$$h = \frac{\int (c_p T) d\dot{m}}{\int d\dot{m}} \quad (3.1)$$

$$h = \frac{\sum_{i=1}^{48} (c_p T A \mathbf{r})_i}{\bar{c}_p \bar{\mathbf{r}} A_{total}} \frac{v}{v} \quad (3.2)$$

4. Exhaust Temperature

The exhaust temperature measurements are taken at four locations, two from each of the two exhaust stacks. Different temperature profiles were observed when the PT speed was varied while the GGT speed remained constant. At the highest PT speed, one of the measurements was considerably higher than the other three. At the lowest PT speed, the same behavior was seen but the peak temperature was in the other exhaust stack.

C. INSTRUMENTATION REQUIREMENTS

Accurate temperature and pressure measurements before and after each major component are necessary for producing a representative cycle graph. Mass flow measurements for air and fuel are needed to calculate power and energy balances. The following measurements for the 250-C18 gas turbine are needed for a thorough analysis of the engine and the instrumentation package.

- | | | |
|------------------------|----------|-------------|
| 1. Air Mass Flow Rate | [lbm/s] | \dot{m}_a |
| 2. Fuel Mass Flow Rate | [lbm/hr] | \dot{m}_f |

3. Compressor/GGT Speed	[rpm]	N ₁
4. Power Turbine Speed	[rpm]	N ₂
5. Compressor Inlet Total Temperature	[°R]	T _{t2}
6. Compressor Inlet Total Pressure	[psia]	P _{t2}
7. Compressor Inlet Static Pressure	[psia]	P ₂
8. Compressor Discharge Total Temperature	[°R]	T _{t3}
9. Compressor Discharge Total Pressure	[psia]	P _{t3}
10. Gas Generator Inlet Total Temperature	[°R]	T _{t4}
11. Gas Generator Inlet Total Pressure	[psia]	P _{t4}
12. Power Turbine Inlet Total Temperature	[°R]	T _{t5}
13. Power Turbine Inlet Total Pressure	[psia]	P _{t5}
14. Exhaust Total Temperature	[°R]	T _{t7}
15. Exhaust Static Pressure	[psia]	P ₇
16. Torque	[ft-lb]	τ
17. Shaft speed	[rpm]	N ₃
18. Output Power	[SHP]	P _{out}

THIS PAGE INTENTIONALLY LEFT BLANK

IV. INSTRUMENTATION IMPROVEMENTS

A. PRESSURE SENSOR SYSTEM REPLACEMENTS

The hardware improvements with the instrumentation package involved the pressure measurements. The Scanivalve DSA 3017 pressure sensor has the ability to compare sixteen channels to an isolated reference pressure within a single package. The DSA 3017 also has the ability to continually take data over a period of time and give an average. It is temperature compensating and vibration tested, which means it can be mounted on the engine stand to minimize distance between the measurement locations and the sensor. Since the connection is ethernet based, the data is processed on a PC, which is connected to the sensor with ethernet cables that are not affected by the gas turbine engine. Due to the various pressure ranges throughout the system, three different measurement scales were used to maximize accuracy: 10" H₂O, 2.5 psid, and 100 psid. A Mystic barometer is used to measure the absolute ambient pressure, this measurement value will be used as a reference for each of the DSA 3017 pressure sensors.



Figure 4.1. Scanivalve DSA 3017 Pressure Sensor

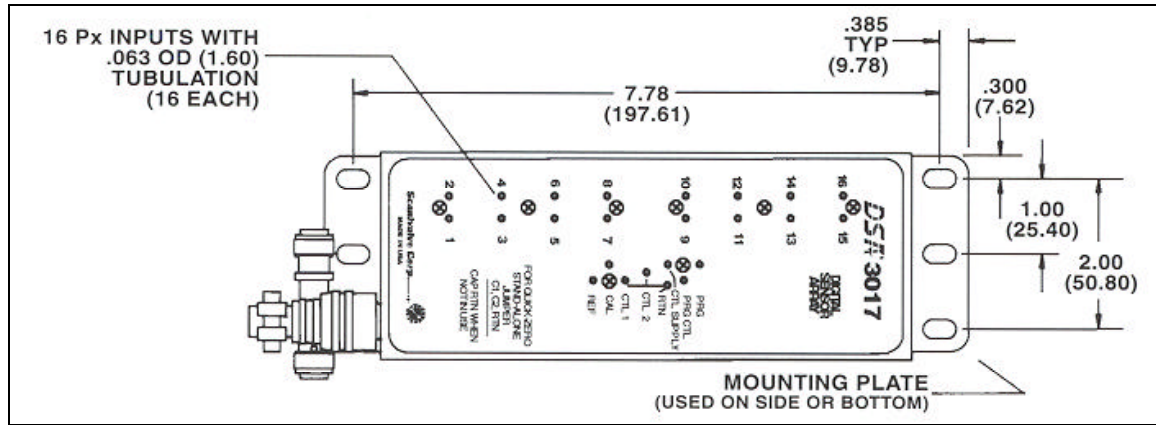


Figure 4.2. DSA 3017 Schematic [Top View]

Table 4.1. Pressure Sensor Locations

Pt	Difference Range			DSA 3017	10"H ₂ O	2.5 psid	100 psid
				# of channels used			
Amb	0	reference			1	1	1
Cell	1	"H ₂ O			1	1	1
2	7.5	"H ₂ O			1	1	1
3	78	psid					2
4	73	psid					2
5	15	psid					2
7	9	"H ₂ O			2	2	2
Pt2-P2	1.4	psid				1	1

Pressure sensors were connected to the pressure probes installed in the calibrated bellmouth at the compressor inlet. An air mass flow calculation can be made and compared to the value measured by the dynamometer's two turbine flow meters.

$$\dot{m}_a = \frac{C_d A P_{t_2}}{\sqrt{R T_{t_2}}} \sqrt{\frac{2k}{k-1} \left(\frac{P_2}{P_{t_2}} \right)^{\frac{2}{k}} \left[1 - \left(\frac{P_2}{P_{t_2}} \right)^{\frac{k-1}{k}} \right]} \quad (4.1)$$

Table 4.2. Temperature Sensor Locations

Tt		# of measurements
Amb		1
Cell		1
2		2
3		2
4		48
5		2
7		4

B. IMPLEMENTATION

The DSA 3017 required 0.063” OD tubing for the connection between the pressure probes and the pressure sensor. The high temperatures experienced within the gas turbine engine would melt the nylon connection tubing and damage the DSA 3017; therefore the pressure probes were extended with four feet of steel tubing. This would allow the air to cool before entering the connection tubing and pressure sensor. The signal is then processed on a PC.

C. TEMPERATURE INSTRUMENTATION

The temperature measurement system was not modified because the measurement data was within a 1-2% difference from the calibrated model. It appeared that the thermocouples were placed at appropriate locations within the flow and were reading realistic temperature values based on the installation design manual. The same temperature data acquisition system was used because a time resolved temperature measurement would not show significant fluctuations.

The temperature instrumentation was also used to analyze the flow at certain state points. The thermocouples within the instrumentation ring at the gas generator turbine inlet were mapped out on a representation of the annulus so the temperature measurements could be seen on a contour plot. This contour plot could be used to compare the profile factor with the physical orientation of the annulus and the relative

location of the compressor discharge inlets. This comparison could contribute to an analysis on how the flow field affects the temperature measurements.

A visual model was also made to analyze the temperature measurements at the power turbine exit. The model compares the temperature differences between the two exhaust stacks at different power turbine speeds. The temperature profile at the power turbine exit was used to analyze how the power turbine rotor stages could affect the annulus temperature profile from the gas generator turbine inlet.

V. RESULTS AND EVALUATION

Measurement data were collected from an engine test with the improved instrumentation scheme. The test was performed at a maximum power setting with the GGT speed at 51,120 RPM and the PT speed at 35,000 RPM. Temperature and pressure measurements will be compared with values supplied by the SF-901 dynamometer and the Allison installation design manual.

A. KEY PARAMETERS

Table 5.1. Key parameter comparison

		ma [lb/s]	ma [lb/s]	mf [lb/hr]	Output [SHP]
		Bellmouth	dyno	dyno	
Predicted Values		3.02	3.02	202.54	285.94
Measured Values		3.07	3.19	205.67	282.10
Difference		1.71%	5.71%	1.55%	-1.34%

Table 5.1 shows that the key parameter measurements like air mass flow rate, fuel mass flow rate, and output shaft horsepower have less than 3% difference from the calibrated model values. The measurement of air mass flow from the dynamometer exceeds the 3% difference margin, which required an accurate value for vapor pressure to be manually inputted into the dynamometer. The inaccurate measurement of volumetric airflow rate could have been the result of an incorrect vapor pressure input.

B. STATE POINT MEASUREMENTS

Table 5.2. State point comparison

	T _{t2}	T _{t3}	T _{t4}	T _{t5}	T _{t7}	P _{t2}	P _{t3}	P _{t4}	P _{t5}	P _{t7}
	[R]	[R]	[R]	[R]	[R]	[psia]	[psia]	[psia]	[psia]	[psia]
Predicted Values	535.0	980.0	2232.7	1830.0	1565.2	14.59	83.98	78.10	29.64	14.70
Measured Values	534.6	986.8	2286.9	1815.1	1537.8	14.59	82.08	79.81	30.10	14.80
Difference	-0.08%	0.69%	2.43%	-0.81%	-1.75%	-0.04%	-2.26%	2.19%	1.57%	0.68%

C. GAS GENERATOR TURBINE INLET TEMPERATURE PROFILE

The temperature profile was neither uniform nor symmetrical. Due to the temperature profile and its wide range of temperatures, it was assumed that there was a problem with the thermocouple configuration. After a discussion with Scott Wood, a Model 250 test engineer at Rolls Royce, it was determined that this particular engine was producing measurements similar to those produced at the Rolls Royce labs. The temperature profile presented is suspected to be a result of the uneven mass flow between the two compressor discharge ducts. The airflow may be directing the combustor flame toward one side of the thermocouple ring. The hot spot is toward the side with the compressor duct having the lower pressure. The difference between the gas generator turbine inlet temperatures calculated from a fuel based energy balance is only 2.43% higher from the mass based calculated value, assuming constant axial velocity.

When plotting the profile factor around the annulus, a difference can be seen when comparing the profiles from different gas generator turbine speeds. At 80% of maximum speed, the hot area of the annulus occupies the left side, and as speed increases to 100%, the hot area occupies only the top left corner of the annulus.

$$PF = \frac{T - T_{\min}}{T_{\max} - T_{\min}} \quad (5.1)$$

Table 5.3. Gas generator turbine inlet temperature comparison @ full power

	$T_{t4}[R]$
TC Average	2310.2
Mass Based	2286.9
Fuel Based	2232.66

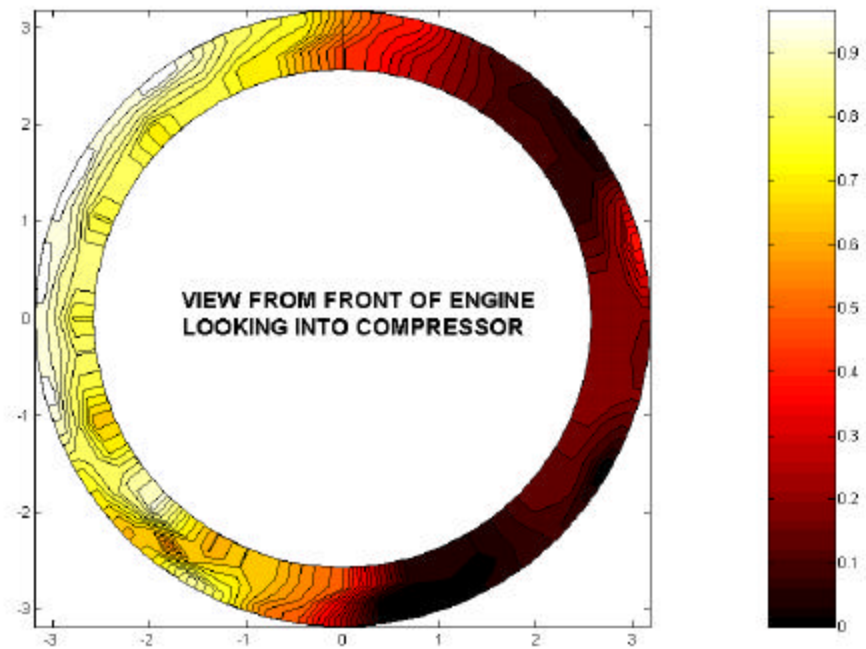


Figure 5.1. Gas generator turbine inlet profile factor @ 80% of maximum compressor speed

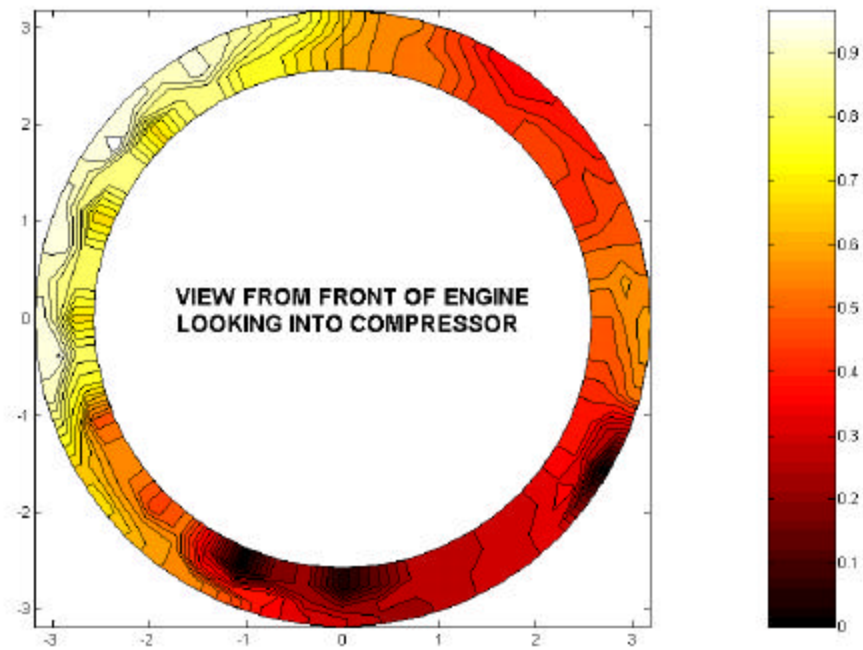


Figure 5.2. Gas generator turbine inlet profile factor @ 100% of maximum compressor speed

The scale for the contour plots consisted of 30 divisions. The lines on the plot separate color fields that represent a difference of 0.033.

D. EXHAUST TEMPERATURE

The temperatures at the power turbine exit changed with power turbine speed at a constant compressor speed. At lower speeds, the maximum temperature measurement was in the left exhaust stack, but as speed increased, the higher temperature measurements were measured in the right stack. Figure 5.3 shows how the temperature profile changes. The two left columns in each set represent the temperature measurements in the left exhaust stack, and the two right columns represent the measurements from the right stack.

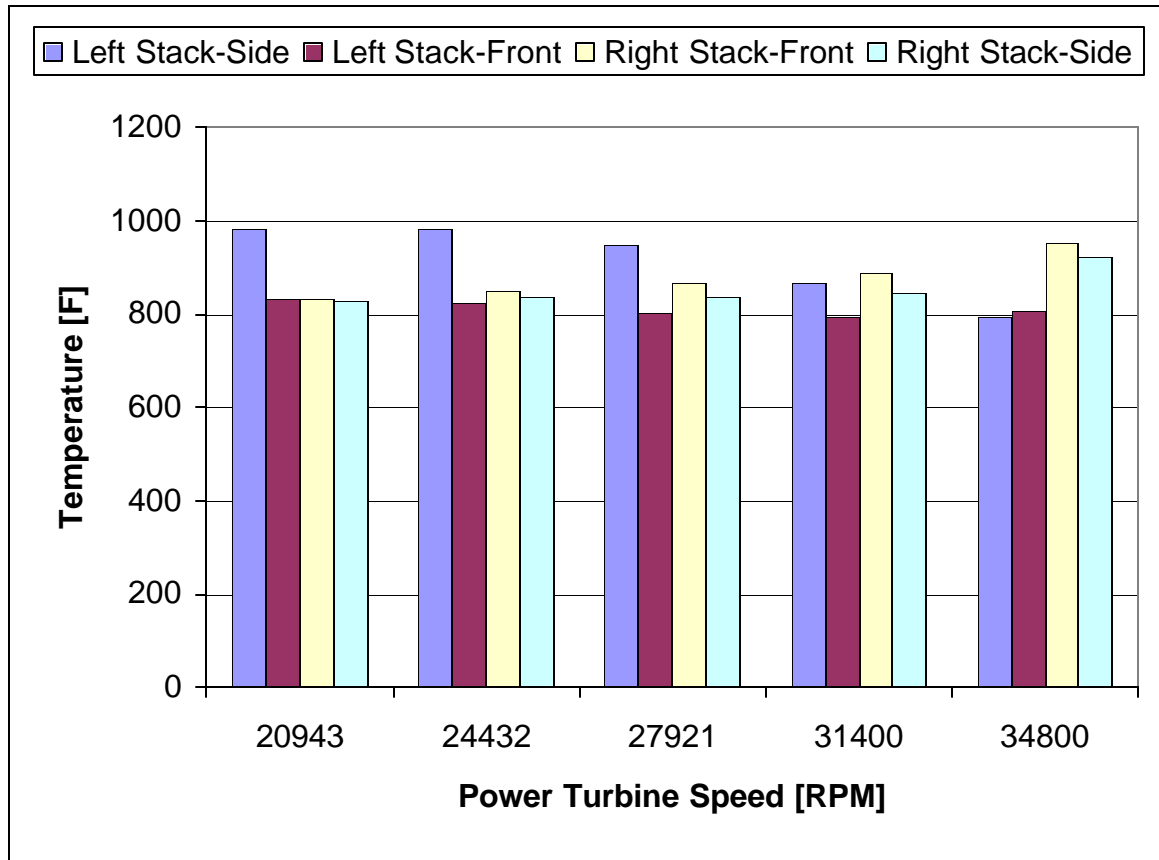


Figure 5.3. Power turbine exit temperature measurements at constant gas generator turbine speed for 5 different power turbine speeds

E. PRESSURE MEASUREMENTS

Pressure measurements were taken throughout the engine at one-second intervals. The data were used to plot the pressure fluctuations over time. The y-axis in each plot represents the pressure difference from the average measurement value and the x-axis represents time.

The pressure probes in each of the compressor discharge ducts experienced similar temporal pressure variations. The compressor seems to be affecting the discharge pressure on both sides evenly. The pressure probes at the top and bottom of the gas generator turbine inlet were also experiencing similar fluctuations. The temporal pressure fluctuations at the gas generator turbine inlet were similar between the top and bottom halves. The pressure fluctuations at the compressor discharge are similar to the average pressure fluctuations at the gas generator turbine inlet. It appeared that the

pressure variations at the gas generator turbine inlet are caused primarily by the compressor speed fluctuations.

Figure 5.6 was used to analyze the affect of the compressor discharge pressure variations on compressor adiabatic efficiency assuming the temperature ratio remained constant. Table 5.4 shows that there is a 2% difference in adiabatic efficiency between the values based on the maximum and minimum fluctuations.

Table 5.4. Compressor adiabatic efficiency comparison

	P_{t3}	η_c
avg	80.02	75.45%
max	80.42	75.72%
min	79.62	73.78%

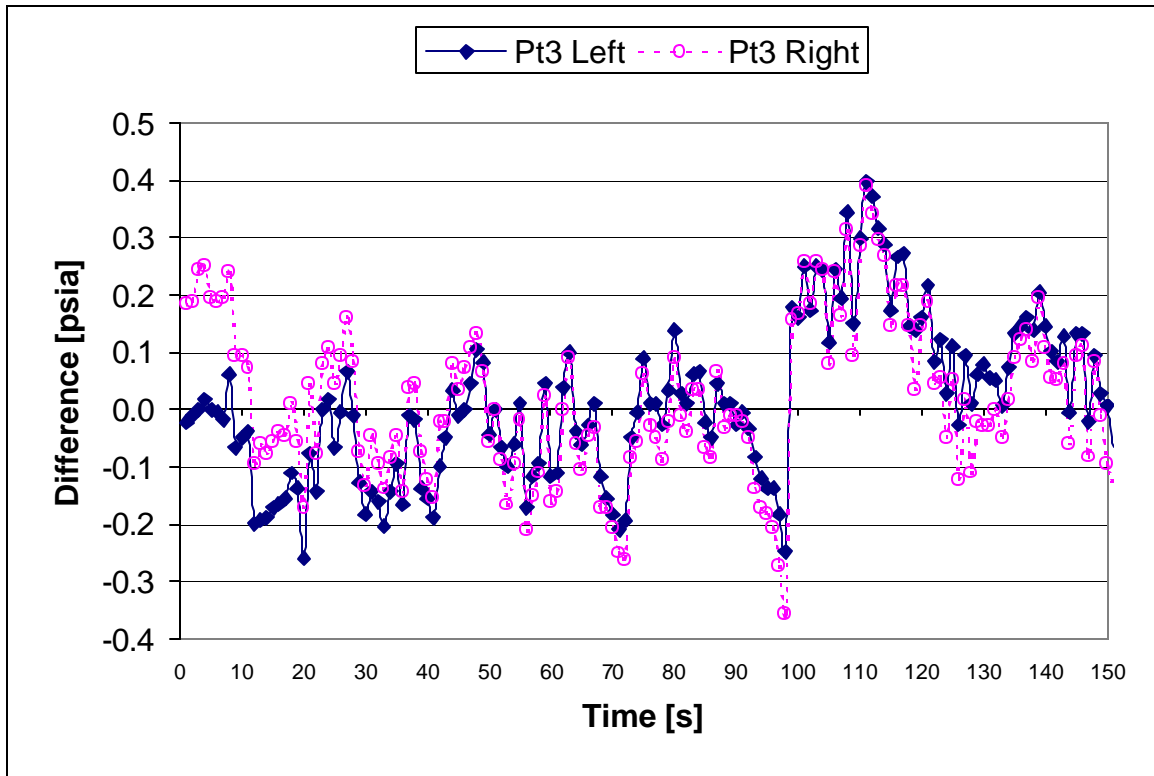


Figure 5.4. Compressor discharge pressure measurement fluctuations

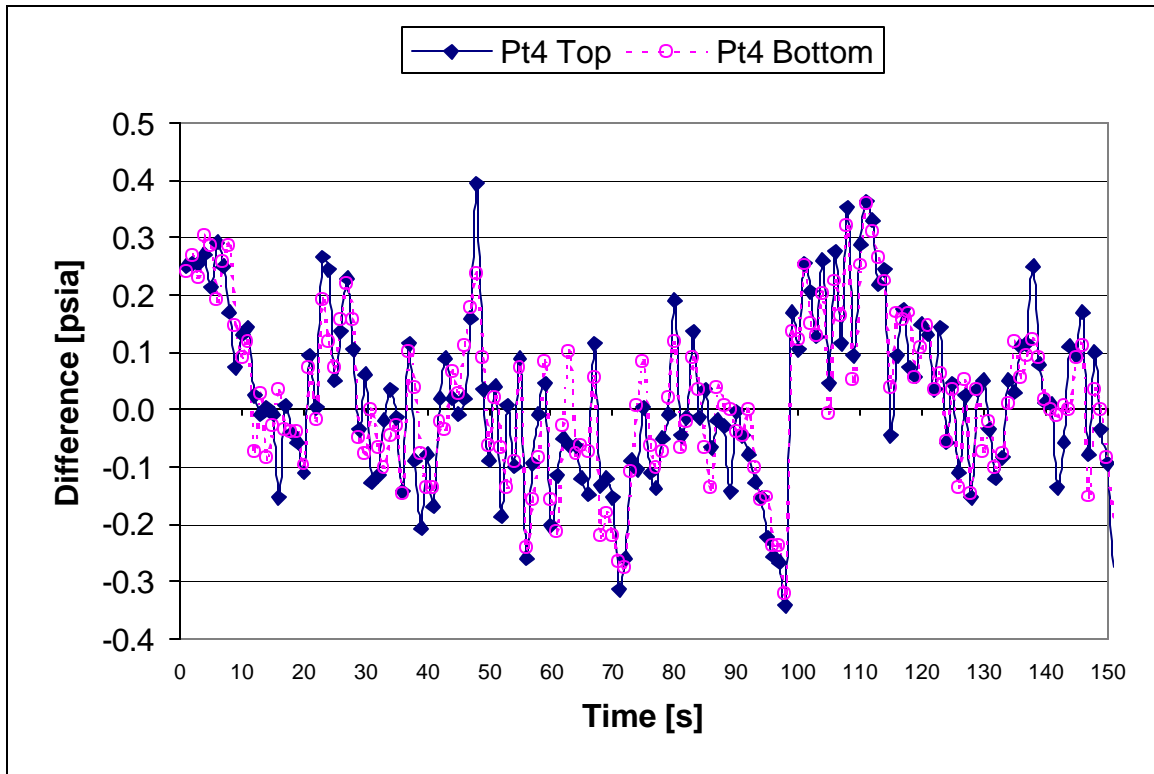


Figure 5.5. Gas generator inlet pressure measurement fluctuations

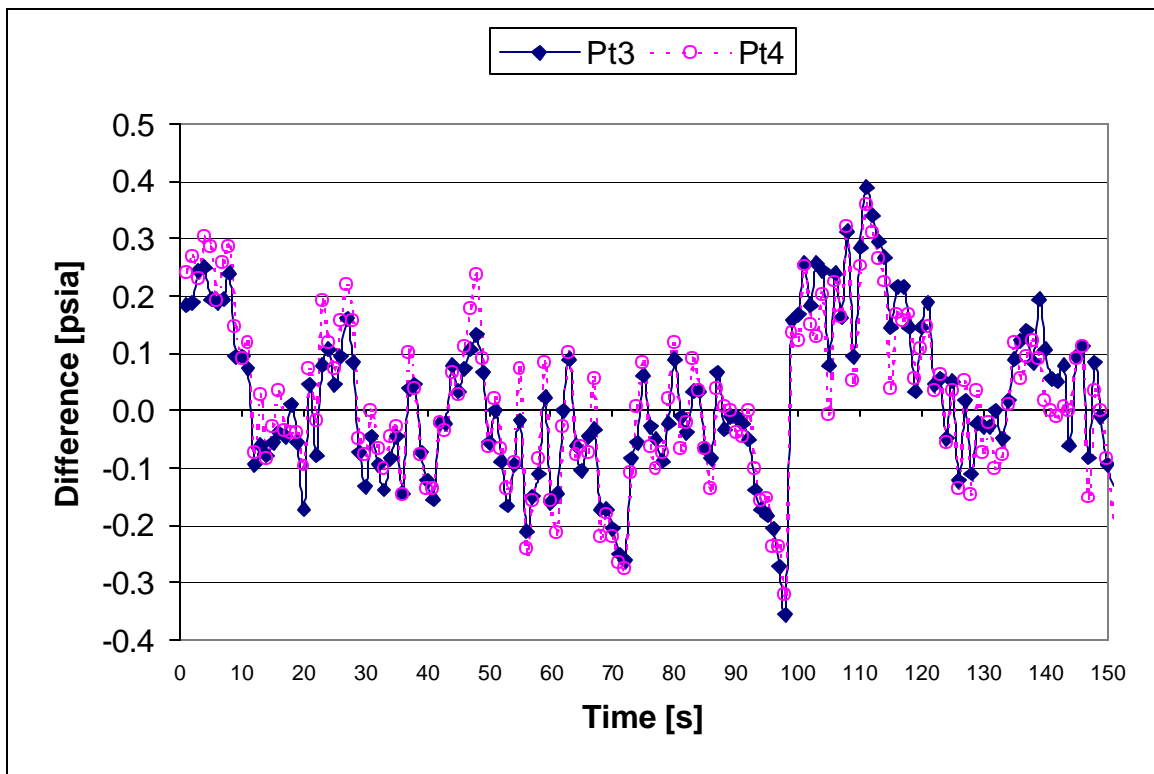


Figure 5.6. Compressor discharge and gas generator inlet pressure measurement fluctuation comparison

THIS PAGE INTENTIONALLY LEFT BLANK

VI. SUMMARY, CONCLUSIONS AND RECOMMENDATIONS

A. SUMMARY

The preexisting flow-path instrumentation was evaluated and it was determined that there existed several problems in the measurement system, including inaccurate measurement of airflow rate, fuel flow rate, and output power. These parameters varied as much as 10-15% from expected values. Also, several quantities that are useful in describing the environment in which the engine operates, such as the inlet pressure depression, were not measured. To improve measurement quality and to obtain previously unknown pressures, new pressure measuring instrumentation was installed. Finally, the calibrated bellmouth flow meter was instrumented to provide a redundant measurement of inlet air mass flow to the engine.

A primary flow path thermodynamic model of the engine was developed and calibrated to match the major output quantities and thermodynamic states between components for standard ISO conditions at full power. This model was then used to predict the total pressures and temperatures between the components and the primary output of the engine under the conditions under which the engine operates in the cell. These predictions were used to evaluate the accuracy of the measurements.

B. CONCLUSIONS

The following conclusions on the accuracy of the upgraded flow path measurements have been drawn based on the consistency of the measured data and comparisons of these quantities to the values predicted by the calibrated thermodynamic model:

1. The installation of the digital scanning array (DSA) pressure measurement sensors increased the accuracy at the existing measurement locations and provided additional useful data. The pressure measurements are generally consistent with the predictions from the thermodynamic model and expectations; the measured values were within 3% of expected values. However, the combustor total pressure loss was measured

to be about 3%, which seems low for a small, reverse flow burner. Pressures measured in similar locations, e.g. from the left and right side, are in agreement to within a fraction of a psi and all measurements are repeatable from run to run, which are an indicator of high quality data.

2. Temporal fluctuations in the measured pressures, defined by the time resolved measurement minus the average value at that location, from all channels after the compressor were very similar, with peak-to-peak variations on the order of 0.7 psid. These variations are presumably due to small variations in compressor speed. While a systematic evaluation of the sample interval or record length needed to obtain repeatable pressure averages were not done, it seems that a 30 second record with sampling interval of one second is sufficient to obtain repeatable averages to within a couple of tenths of a psi, if the compressor speed is relatively constant.

3. The bellmouth provides a measurement of air mass flow that is more consistent with predicted values than the dynamometer's turbine flow meters. The bellmouth calculation produced a 1.71% difference from the expected value while the dynamometer measurement had a difference close to 6%

4. The temperatures measured with the thermocouples do not agree closely with predicted values in the engines hot section. Specifically, the mass averaged calculation of the turbine inlet temperature, T_{T4} , based on the 48 thermocouple measurements and an assumed constant axial velocity for the gas generator inlet temperature is about 50 degrees F higher than the value from the engine model or a combustor energy balance. Also, the power turbine exit temperature is about 30 degrees lower than an expected value. The temperature profile at the power turbine exhaust is the result of the temperature profile at the gas generator turbine inlet and the swirl produced by the power turbine. The hot spot in the gas generator turbine inlet temperature profile is being directed toward one of the exhaust stacks, depending on the power turbine speed.

5. The temperature profile out of the combustor was not axis-symmetric at any power setting. At lower power settings (e.g. 80%) there were hotter and cooler halves, about the vertical axis of symmetry, which may be due to the slightly higher pressure entering the left side of the combustor pushing the "fireball" to the right side of the

annulus. However, at the 100% power setting, the profile factor lost its symmetry and the highest temperatures were in the upper left-hand corner. This change in the nature of the temperature field is not understood.

C. RECOMMENDATIONS

There are several remaining problems and uncertainties with the measurement system, which should be addressed. The major problem is that of relatively large uncertainties in the temperature measurements in the three hot section locations. The reason(s) that the mass averaged turbine inlet temperature, as calculated with the thermocouple measurements, do not match the temperature calculated from a combustor energy balance should be determined. Since the spatial resolution seems adequate, other reasons should be investigated, such as the thermocouples not properly reading the gas temperature due to radiation loading, etc. The two thermocouples used in the measurement of power turbine inlet temperature, and the four used for the exit temperature are probably not sufficient to provide adequate spatial resolution for the calculation of a representative average temperature. The pressure probes at the power turbine inlet should be replaced with the same temperature/pressure combination devices at the compressor discharge. A more detailed survey of the outlet temperature versus power turbine speed at a constant engine mass flow should be conducted to determine how an accurate average outlet temperature should be measured.

Finally, an evaluation of the effects of the instrumentation that measures the gas generator inlet conditions should be made. The 50 probes may be conducting heat away from the air while increasing pressure losses.

THIS PAGE INTENTIONALLY LEFT BLANK

APPENDIX A. DSA 3017 SPECIFICATIONS

Specifications											
Inputs (Px):											
DSA3017:	Standard: 16 each .063 inch (1.6mm) O.D. tubulations										
DSA3018:	Standard: 1/8 inch Swagelok fittings Optional: 1/16 and 1/4 inch Swagelok fittings										
Full Scale Ranges:											
Differential:	±10 inch H ₂ O, 1, 2.5, 5, 15, 30, 50, 100, 250, 500, 600, 750 psid										
Absolute:	15, 30, 50, and 100 psia										
Accuracy: (Including linearity, hysteresis, and repeatability)	<table border="1"> <thead> <tr> <th>Sensor Pressure Range</th><th>Static Accuracy (% F.S.)</th></tr> </thead> <tbody> <tr> <td>±10 inch H₂O (2.5 kPa)</td><td>±.20%</td></tr> <tr> <td>±1, ±2.5 psid</td><td>±.12%FS</td></tr> <tr> <td>±5 to 500 psid</td><td>±.05%</td></tr> <tr> <td>±501 to 750 psid</td><td>±.08%</td></tr> </tbody> </table>	Sensor Pressure Range	Static Accuracy (% F.S.)	±10 inch H ₂ O (2.5 kPa)	±.20%	±1, ±2.5 psid	±.12%FS	±5 to 500 psid	±.05%	±501 to 750 psid	±.08%
Sensor Pressure Range	Static Accuracy (% F.S.)										
±10 inch H ₂ O (2.5 kPa)	±.20%										
±1, ±2.5 psid	±.12%FS										
±5 to 500 psid	±.05%										
±501 to 750 psid	±.08%										
Resolution:	16 bit										
Scan Rate:	200 samples/channel/second max. 3.2kHz/DSA module up to 250kHz with Ethernet system										
Communication:	Ethernet 10base2 (standard) Ethernet 10baseT (optional) RS232 RS485 (contact factory)										
Communication Protocol:	TCP/IP 45Hz/channel EU										
Operating Temperature:	DSA3017: 0°C to 60°C DSA3018: -55°C to 60°C										
Temperature Compensated Range:	0°C to 60°C standard										
Mating Connector Type:	I/O: RG-58 BNC or RJ-45 Power: Bendix PTO2A-8-3P, 3 pin female Trigger: Bendix PTO2A-8-6P, 6 pin female										
Power Requirements:											
DSA3017:	28Vdc nominal @ 350mA (20-36Vdc)										
DSA3018:	28Vdc nominal @ 1.2A (24-36Vdc)										
External Trigger:	6 mA at 4 Vdc minimum edge sensing										
Overpressure Capability:	10 inch H ₂ O = 2 psi (13.79kPa) 1 psid = 5 psi (35kPa) 200 psid (1725kPa) = 200% 500 psid (3500kPa) = 150% 600 psid (4200kPa) = 125% 750 psid (5250kPa) = 100%										
Maximum Reference Pressure:	250 psig (1724kPa) (Consult factory for higher reference pressures)										
Media Compatibility:	Gases compatible with silicon, silicone, aluminum, and Buna-N										
Weight:	DSA3017/16Px: 6.4 lbs. (2.9 kg) DSA3018/16Px: 9.8 lbs. (4.45 kg)										
Total Thermal Error over 0 - 60°C Range:	±.001% F.S./°C										

Figure A.1. DSA 3017 Specifications

THIS PAGE INTENTIONALLY LEFT BLANK

APPENDIX B. MATLAB CODE FOR GGT INLET TEMPERATURE PROFILE

```
clear
rv=[2.573 2.78 2.95 3.1 3.18];
thv=linspace(pi/2,5*pi/2,49);
[r,th]=meshgrid(rv,thv);
x=r.*cos(th);
y=r.*sin(th);
a=h(:,1);
b=h(:,3);
z=[a h b];
contourf(x,y,z,30)
colorbar
axis square
```

THIS PAGE INTENTIONALLY LEFT BLANK

APPENDIX C. COLLECTED DATA

The following tables contain data collected and the average values used for thermodynamic calculations. The engine conditions were 100% compressor speed and 100% power turbine speed. The unit for temperature is Rankine, and the unit for pressure is pounds per square inch absolute.

Table C.1. Temperature and pressure data

[R]										
T _{t2}	536.5		T _{t4ir}	2407.8		T _{t4mr}	2496.0		T _{t4or}	2474.7
T _{t2}	532.7		T _{t4ir}	2376.2		T _{t4mr}	2510.4		T _{t4or}	2478.6
T _{t2avg}	534.6		T _{t4ir}	2371.9		T _{t4mr}	2492.0		T _{t4or}	2477.2
T _{t3}	986.7		T _{t4ir}	2376.1		T _{t4mr}	2498.3		T _{t4or}	2477.2
T _{t3}	986.9		T _{t4ir}	2289.8		T _{t4mr}	2346.6		T _{t4or}	2376.2
T _{t3avg}	986.8		T _{t4ir}	2274.8		T _{t4mr}	2331.6		T _{t4or}	2320.8
T _{t4mass avg}	2286.9		T _{t4ir}	2069.1		T _{t4mr}	2256.3		T _{t4or}	2213.3
T _{t5}	1815.1		T _{t4ir}	2088.3		T _{t4mr}	2184.9		T _{t4or}	2179.2
T _{t7}	1633.6		T _{t4ir}	2187.1		T _{t4mr}	2203.0		T _{t4or}	2205.6
T _{t7}	1511.2		T _{t4ir}	2209.0		T _{t4mr}	2238.7		T _{t4or}	2073.4
T _{t7}	1488.0		T _{t4ir}	2243.2		T _{t4mr}	2283.7		T _{t4or}	2328.1
T _{t7}	1518.4		T _{t4ir}	2296.5		T _{t4mr}	2331.2		T _{t4or}	2295.0
T _{t7avg}	1537.8		T _{t4ir}	2262.6		T _{t4mr}	2270.3		T _{t4or}	2243.9
			T _{t4ir}	2274.5		T _{t4mr}	2236.5		T _{t4or}	2234.5
			T _{t4ir}	2297.1		T _{t4mr}	2303.8		T _{t4or}	2322.0
			T _{t4ir}	2338.3		T _{t4mr}	2402.3		T _{t4or}	2442.9

[psia]									
P_{tamb}	14.681	P_{t3left}	82.126	P_{t4top}	79.788	P_{t5}	29.987	P_{t7left}	14.769
P_{t2}	14.591	$P_{t3right}$	81.914	$P_{t4bottom}$	79.826	P_{t5}	30.183	$P_{t7right}$	14.729
P_2	12.985	P_{t3avg}	82.020	P_{t4avg}	79.807	P_{t5avg}	30.085	P_{t7avg}	14.749

THIS PAGE INTENTIONALLY LEFT BLANK

LIST OF REFERENCES

1. Allison Gas Turbines, *Model C-18 Installation Design Manual*, 1976.
2. White, Frank M., *Fluid Mechanics*, pp.587, Mcgraw-Hill, Inc., 1999.
3. Haas, David W., *Instrumentation Design and Control of a T63-A-700 Gas Turbine Engine*, June 1996.
4. Eckerle, Brian P., *Design and Component Integration of a T63-A-700 Gas Turbine Engine Test Facility*, September 1995.
5. Superflow Corporation, *SF-901 Instruction Manual*, 1993.
6. Point of Contact Tom Christian, Electronic / Computer systems engineer, Naval Postgraduate School – Code ME/CS, 700 Dyer Road, Monterey, CA 93943-5100, PH: (831) 656-3208, May 2002.
7. Point of Contact Louis Harris, Scanivalve Corporation, Customer Service Representative, 1722 N. Madson St, Liberty Lake, WA 99019, PH (800) 935-5151, April 2002.
8. Point of Contact Scott Wood, Allison Rolls Royce Corporation, Test Engineer, P.O. Box 420, Indianapolis, IN 46206-0420, PH (317) 230-3459.

THIS PAGE INTENTIONALLY LEFT BLANK

INITIAL DISTRIBUTION LIST

1. Defense Technical Information Center
Ft. Belvoir, Virginia
2. Dudley Knox Library
Naval Postgraduate School
Monterey, California
3. Department Chairman, Code ME
Department of Mechanical Engineering
Naval Post Graduate School
Monterey, California 93943-5000
4. Professor Knox T. Millsaps Code ME/Ps
Department of Mechanical Engineering
Naval Post Graduate School
Monterey, California 93943-5005
5. Curricular Officer, Code 34
Department of Mechanical Engineering
Naval Post Graduate School
Monterey, California 93943-5100
6. Mr. Tom Christian
Department of Mechanical Engineering
Naval Post Graduate School
Monterey, California 93943
7. Mr. Scott Wood
Allison Rolls Royce Co.
P.O. Box 420
Indianapolis, Indiana 46206-0420
8. Mr. Louis Harris
Scanivalve Co.
1722 North Madson St.
Liberty Lake, WA 99019
9. ENS Kenneth C Bruan
13052 Exinite Ct.
Reno, NV 89506